



# Damage Estimation in Masonry Buildings Based on Excavation-Induced Ground Movements

Ibrahim Naeimifar · Shahaboddin Yasrobi · Ali Akbar Golshani · Mehdi Joneidi

Received: 25 June 2019 / Accepted: 14 February 2021 / Published online: 20 March 2021  
© The Author(s), under exclusive licence to Springer Nature Switzerland AG 2021

**Abstract** Excavation-induced ground movements and the resulting damages to adjacent structures and facilities is a source of concern for excavation projects in urban areas. The concern will be even higher if the adjacent structure is old or has low strength parameters like masonry building. Frame distortion and crack generation are predictors of building damage resulted from excavation-induced ground movements, which pose challenges to projects involving excavations. This study is aimed to investigate the relation between excavation-induced ground movements and damage probability of buildings in excavation affected distance. The main focus of this paper is on masonry buildings and excavations stabilized using soil nail wall method. To achieve this purpose, 21 masonry buildings adjacent to 12 excavation projects were studied. Parametric studies were performed by developing 3D FE models of brick walls and excavations stabilized using soil nail wall. Finally, probability evaluations were conducted to analyze the outputs obtained from case studies. Based on the obtained results, simple charts were established to estimate the damage of masonry structures in excavation affected

distance with two key parameters including “Displacement Ratio” and “Normalized Distance”. The results also highlight the effects of building distance from excavation wall on its damage probability.

**Keywords** Excavation · Ground movements · Building · Damage · Probability · Finite element

## Abbreviations

BW	Brick wall
DPI	Damage potential index
DR	Displacement ratio
EAD	Excavation affected distance
EIGM	Excavation-induced ground movement
ND	Normalized distance
SNW	Soil nail wall
TMS	Twenty one masonry structures

## 1 Introduction

Progressive ground movements induced by excavation in urban areas increases concerns about surrounding buildings damage and the consequent reconstruction costs. On the other hand, higher values of Excavation-Induced Ground Movement (EIGM) result in smaller values of ground pressure on the support wall that, in turn, leads to more economic design of support structures. So, proper prediction of building damage

---

I. Naeimifar (✉)  
Department of Civil Engineering, Hashtgerd Branch,  
Islamic Azad University, Hashtgerd, Alborz, Iran  
e-mail: i.naeimifar@yahoo.com

S. Yasrobi · A. A. Golshani · M. Joneidi  
Department of Civil Engineering, Tarbiat Modares  
University, Tehran, Iran

due to EIGM results in more accurate estimation of costs involved in excavation project. Typically, EIGM is evaluated by assessment of excavation wall deformations (Lazarte et al. 2003; Yoo and Lee 2008). Evaluation of settlement profile in surrounding area, basal heave and mode of wall deformation might be potentially considered for assessing ground movement (Chang et al. 2011; Zhang et al. 2014; Sun et al 2005; Korff et al. 2016) and they are depended on different parameters such as soil properties (Singh and Babu 2010; Wu et al 2013). To characterize the damage that structure has experienced through EIGM, “damage level” is generally used as a term defining the limiting conditions of expected damage in buildings according to EIGM. Damage levels have been investigated and developed for buildings adjacent to excavations by performing physical scaled model tests (Ou et al. 2000; Sawwaf and Nazir 2011), analytical approaches (Halim and Wong 2011; Basmaji 2019), field observations, case studies (Son and Cording 2005), 2D numerical analyses (Son and Cording 2005, 2011; Hashemi et al 2015), and also 3D numerical simulations (Minh 2013; Lin et al. 2014a, b; Orazalin et al. 2015; Zhang et al. 2016; Dong et al. 2017). To classify damage levels in buildings, different methods are also addressed in literature by focusing on the ground surface settlement and horizontal strain of building frames (Ghahreman 2004), differential settlement of building frames (Halim and Wong 2011), and lateral strain and angular distortion of building walls (Schuster et al. 2009). Probabilistic framework was also interested by researchers for evaluation of damage probability of buildings in Excavation Affected Distance (EAD) due to the uncertainties involved in parameters affecting the EIGM and the resulting building damages, (Goh et al. 2013; Wang et al 2014; Wu et al 2014; Zhang et al. 2015a, b; Su et al. 2017; Zevgolis, and Daffas 2018).

By a review over the literature, various studies can be found on assessment of building damage level based on its distortion in the framework of deterministic or probabilistic analysis. However, dependency of building damage upon EIGM seems to be a difficult issue to be addressed by geotechnical engineers. Nevertheless, in most of projects estimation and inspection of EIGM is more feasible than buildings distortion. The present research seeks to prepare a simple framework for estimation of damage probability in buildings based on excavation wall deflection (as

a predictor of EIGM). The obtained results also establish a better understanding of building damage severity variation in EAD caused by EIGM. The focus of this work is on masonry buildings and excavations stabilized using Soil Nail Wall (SNW) method. Results of paper is more referable when cantilever deformation is the dominant mode of excavation wall deflection.

## 2 Methodology

The steps taken during this study are as follows: 1. Performing case studies; 2. Numerical simulations; and 3. Probability assessments. Investigated parameters, analysis methods, and main outcomes of each step are summarized in Table 1. More details of analysis procedure are presented in the following subsections.

### 2.1 Observational Methods

The most widely accepted and successful way to treat with the uncertainties inherent in dealing with geological materials is the observational method. This method was found that is not feasible in many geotechnical applications to assume very conservative values of the loads and material properties and design for those conditions (Baecher et al. 2005). To determine and classify damage levels in buildings during case studies, observational methods could be applied. One of the most frequently cited method was developed by Burland et al. (1977). Through this method, damage levels are classified based on observed distortion and crack width in the Brick Walls (BWs) of a masonry buildings as shown in Table 2.

Using this method, building damage intensity in EAD could be classified into five levels consists of: Very SLight (VSL), SLight (SL), Moderate (M), SEvere (SE), and Very SEvere (VSE). In the observational method, various signs of damage in different points of a wall result in a damage level for the whole wall. In this research, observational criteria presented in Table 2 were used to assess and classify damage levels for buildings adjacent to excavation area in some parts of case studies.

**Table 1** An over view to different phases of this study

Study steps	Investigated parameters	Method of analyzing	Outcomes
Case studies	Crack width, length, number, and other specifications of buildings damage in EAZ based on site visit + EIGM according to instrumentation results	Observational method offered by Burland et. al. (1977)	Data base consists of excavation instrumentation outputs and damage level of buildings in EAZ
Numerical simulations	Deformation parameters of brick walls + EIGM based on FE models outputs	DPI criterion developed by Schuster et al. (2009)	Extraction of a framework to manage data obtained from case studies to apply effects of damage intensity variation in EAZ
Probability assessments	Probability density functions Cumulative density functions Reliability index	Conditional probability	Assessment of damage probability by neglecting/considering variation of damage intensity in EAZ

**Table 2** Classification of visible damage to walls with particular reference to ease of repair of plaster and brickwork or masonry (Burland 177)

Damage level	Description of typical damage (ease of repair is underlined>)	Crack width (mm)
Very Slight (VSL)	Hairline cracks of than about 0.1 mm are classed as negligible Fine cracks which can easily be treated during normal decoration. Perhaps isolated slight fracture in building. Cracks in external brickwork visible	< 1
Slight (SL)	Cracks easily filled. Redecoration probably required. Several slight fractures showing inside of building. Cracks are visible externally and some repointing may be required externally to ensure weather tightness. Doors and windows may stick slightly	1–5
Moderate	The cracks require some opening up and can be patched by a mason Recurrent cracks can be masked by suitable linings. Repointing of external brickwork and possibly a small amount of brickwork to be replaced. Doors and windows sticking. Service pipes may fracture	5–15 or a number of cracks $\geq 3$
Severe	Extensive repair work involving breaking out and replacing sections of walls, especially over doors and windows. Windows and door frames distorted, floor sloping noticeably. Walls leaning or bulging noticeably, some loss of bearing in beams. Service pipes disrupted	15–25 but also depends on number
Very Severe	This requires a major repair job involving partial or complete re building. Beams lose bearing; walls lean badly and require shoring. Windows broken with distortion. Danger of instability	usually > 25 but depends on number

2.2 DPI Criterion

In correspondence with observational classification developed by Burland et al., Schuster et al. established a computational classification in terms of Damage Potential Index (DPI) as shown in Table 3 (Schuster et al. 2009).

To calculate DPI, Eq. 1, with parameters defined in Eqs. 2–4, is used (Schuster et al. 2009). Based on DPI

formulations, damage levels were depended on wall distortion.

$$DPI = 20000(\epsilon_l \cos^2(\theta) + \beta \sin(\theta) \cos(\theta)) \tag{1}$$

$$\tan(2\theta) = \frac{\beta}{\epsilon_l} \tag{2}$$

$$\beta = (V_1 - V_2)/L \tag{3}$$

$$\epsilon_l = (U_1 - U_2)/L \tag{4}$$

**Table 3** Damage level description based on DPI values (Schuster et al. 2009)

Line	Level of building damage	Damage potential index (DPI)
1	Negligible to very slight	0–15
2	Slight	15–25
3	Slight to moderate	25–35
4	moderate	35–60
5	Sever	60–85
6	Very Sever	> 85

where  $\beta$  is angular distortion,  $\varepsilon_1$  is horizontal gradient, and  $U$  and  $V$  represent the respective horizontal and vertical deformation of predefined points in a Brick Wall (BW) of masonry structure.  $L$  is the distance between mentioned predefined points. These parameters can be obtained using numerical analysis. In this study, DPI criterion pointed out through Eqs. 1–4, were performed to compute and classify damage levels.

### 2.3 Conditional Probability

Applications of probabilistic methods in geotechnical engineering have recently received much attention in recent years. Geotechnical engineers and engineering geologists work with materials with barely known properties and spatial distribution which have loads and resistances coupled often (Baecher et al. 2005). Predicting behavior of buildings adjacent to excavation cannot be made with certainty due to the limited calculation method, limited site exploration, and uncertainties involved soil and buildings parameters. So, in this study, probability evaluations were conducted to analyze the outputs obtained from case studies and numerical models. To assess buildings damage probability in EAD based on EIGM (by focusing on excavation wall deformation in this paper), concept of conditional probability was used. Similar methodology is also referred in literature (Juang et al. 2011; Castaldo et al. 2013; Shi et al. 2013; Goh 2017; Zheng et al. 2018). To achieve the goal, conditional probability of building damage is developed for data obtained from case studies, using Eq. 5.

$$P_D = P[LS] = \sum_y [PL|DR = dr]P[DR = dr] = P_f \times P_{cdf} \quad (5)$$

where  $P_D$  is probability of damage up to a certain level;  $P[LS]$  is conditional probability of building damage for a given “dr”;  $P[DR = dr]$  is probability for occurrence of “dr”; and  $[PL|DR = dr]$  is conditional probability of “dr” in safety margin.  $DR$  is defined in this study as the ratio between maximum wall deflection and Excavation Affected Distance (EAD). According to Hasofer & Lind’s method,  $P_f$  can be calculated using Eq. 6.

$$P_f = \Phi(-\beta) \quad \beta = \frac{\mu}{\sigma} \quad (6)$$

where  $\Phi$  is the standard normal cumulative distribution function;  $\beta$  is Reliability index;  $\mu$  is standard deviation; and  $\sigma$  is average of data in safety margin.

To evaluate  $P_D$ , it is possible to calculate  $P_f \times P_{cdf}$  instead of calculating  $\sum_y [PL|DR = dr]P[DR = dr]$ .

$P_{cdf}$  can be calculated directly from cumulative distribution function, which is derived by integration of probability density function trended through data histogram. By calculating  $P_{cdf}$  from cumulative distribution function and  $P_f$  from Eq. 6,  $P_D$  is obtained using Eq. 5.

### 3 Case Studies

Case studies were performed on 41 excavation projects stabilized by SNW technique and also buildings located in EAD. The cases were obtained from Tehran construction engineering organizations and expert companies. Collected data and measured parameters from case studies are classified into two groups:

1. Data related to SNW specifications, consisting of data from geotechnical investigations in projects location, design album of reinforcement system, supervision reports, and especially instrumentation and monitoring reports.
2. Data related to buildings specifications in EAD, consisting of BWs distance (in masonry buildings) from excavation wall, the number of bays and stories of structures, and especially damage level in BWs during excavation progress based on observational method (Table 2).

Some of the collected data were eliminated from database due to the inaccuracy in the results of monitoring, unfavorable results in displacement caused by nearby galleries or underground facilities, inappropriate execution, non- detectable conditions of buildings in EAD and etc.

For this study, Twenty one Masonry Structures (TMS) adjacent to 12 excavation projects were selected to perform further analysis (29 projects eliminated). The details of TMS data are presented in the “Appendix” and are reported in more details by Naeimifar (2016). The main outputs extracted from case studies are presented in Fig. 1.

In Fig. 1, horizontal axis (Displacement Ratio) shows the ratio between maximum excavation wall displacement and EAD, whereas the vertical axis (Normalized Distance) shows distance of BW from SNW normalized to EAD distance. To determine

maximum wall displacement, monitoring results of projects were used. Distance of BWs from SNW were evaluated using site measurements. In this paper, EAD is defined as the distance from SNW for which the total displacement of ground surface is reduced to 0.1 of maximum SNW deflection. Moreover, EAD for each project is estimated on basis of the performed numerical analysis.

In Fig. 1, label of each point denotes the damage level of BWs in masonry buildings in EAD. For example, label of point “A” represents the damage level equivalent to “Very Slight” (based on Table 2) for a BW (in a masonry building) with a normalized distance equal to 0.75 and displacement ratio equal to 0.0004. As described in part 2.1, based on observational method, damage level is evaluated for whole of a wall. It should be mentioned that all the obtained data (considering displacement ratio and damage level) are related to the final excavation depth. It can be seen from this figure that data are distributed between 0 and 0.003 in displacement ratio and 0 to 0.875 in the normalized distance. Displacement ratio indicates a higher data frequency in the range of 0 to 0.0018. The data presented in the figure are uncertain due to the uncertainties in calculation method, site exploration, and soil and buildings parameters. Because of uncertainties involved in parameters, probability analysis is useful for processing the data. It can be seen from the figure that damage level was increased by displacement ratio increase. The mentioned significant trend in

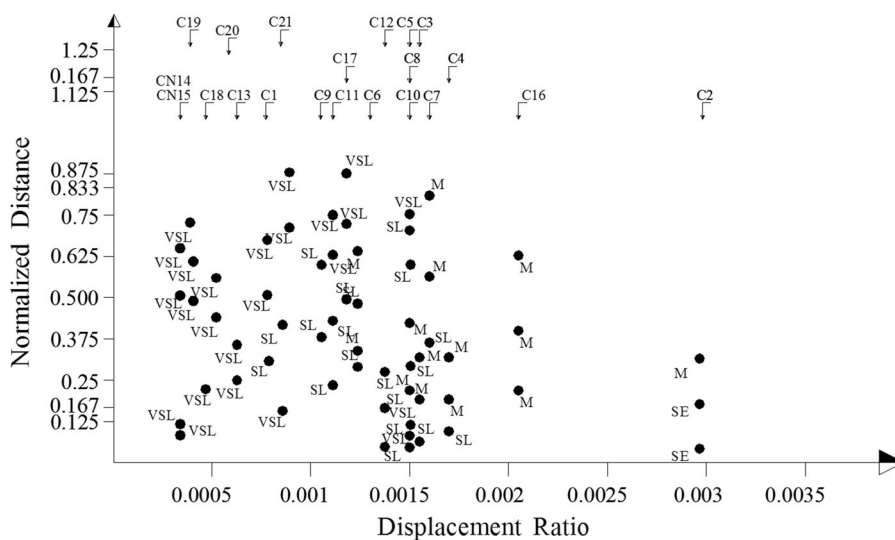


Fig. 1 Observed damage levels of TMS based on displacement ratio and normalized distance

data is a requirement of probability analysis. More details of processing are presented in subsection 2.3 and Sect. 5.

## 4 Development of FE Model

### 4.1 SNW Model

Employing elasto-plastic constitutive laws for SNW components in the framework of finite element formulations, a 3D numerical model of an instrumented excavation project in Tehran was created (Naeimifar 2016). Staged construction process of SNW model is presented in Table 4. Characteristics of elements and constitutive law of FE model are also indicated in Table 5. Table 6 presents the geotechnical situation of project area. Typical views of FE models

and instrumented excavation project are shown in Fig. 2.

The cap plasticity model presented in Table 5 has been widely used in FE modeling of geotechnical applications and consists of three segments (Helwany 2007): a shear failure surface ( $F_S$ ), an elliptical cap ( $F_C$ ), which intersects the mean effective stress axis at a right angle, and a transition region ( $F_T$ ) between these segments introduced to provide a smooth surface. This model can consider the effect of stress history, stress path, dilatancy, and the effect of the intermediate principal stress. Figure 3 shows a schematic representation of the cap model.

To calibrate the FE model, excavation wall deflection predicted using the FE model was compared and verified with the results extracted from the excavation wall monitoring (field results) for different monitoring points (Fig. 4a) on excavation wall. The verification results in Fig. 4b show that the results of present

**Table 4** Staged construction used to develop SNW model

Step no.	Description
1	Creation of model geometry
2	Applying the geostatic stress and loading of BW to the model
3	Resetting displacements in the excavation adjacency to zero
4	Eliminating the first layer of soil elements in the excavation area
5	Activating the nail and shotcrete elements in the first nailing row
6	Repeating steps 4 and 5 to reach excavation bottom level

**Table 5** Type of elements and constitutive models used in FE models

Model label	Type of parts	Type of elements	Constitutive model
SNW	Soil	8-node linear brick	Cap plasticity
	Nail	3-node quadratic beam	Elastic-Perfectly Plastic
	Shotcrete	8-node doubly curved thick shell	Elastic-Perfectly Plastic
BW	Masonry unit	8-node linear brick	Elastic-Perfectly Plastic with Mohr-coulomb surface as yield criteria

**Table 6** Geotechnical situation of project area

Depth (m)	Unit weight ( $\text{kN/m}^3$ )	Cohesion ( $\text{kN/m}^2$ )	Friction angle (Degree)	Elastic modulus ( $\text{kN/m}^2$ )	Poisson ratio
0–1	17.5	5	30	1.5E4	0.35
1–14	19	10	33	6E4	0.3
14-End	19.3	10	35	8E4	0.3

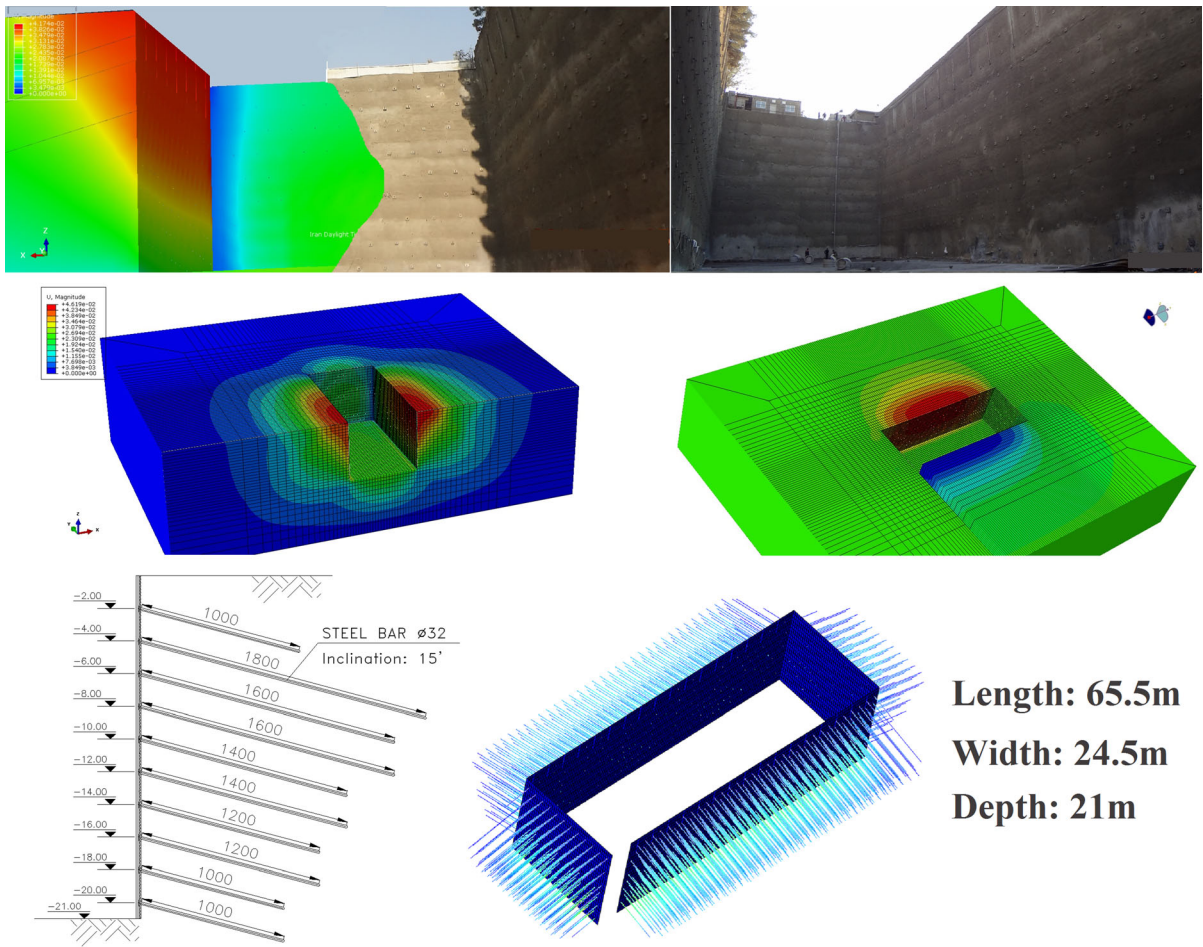


**Fig. 2** Some views of the excavation project performed in calibration of developed SNW models

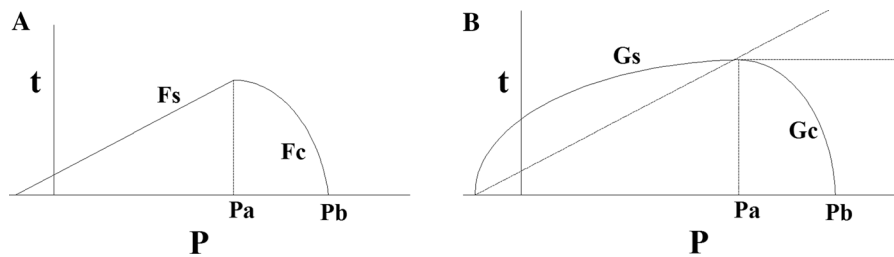


**Fig. 3** Detailed information of the cap plasticity model: **a** yield surfaces in the  $p$ - $t$  plane, And **b** flow potential in the  $p$ - $t$  plane

numerical simulation are in good agreement with the measurements. The observed slight tolerance is within the reasonable range and is attributed to the uncertainty involved in soil properties and monitoring errors.

#### 4.2 BW Model

In this research, also 3D models of an instrumented BW were developed by macro modelling approach. Instrumented BW was constructed on laboratory of Tarbiyat Modares University, Tehran (Shakib et al. 2013). In FE model, masonry unit simulated using

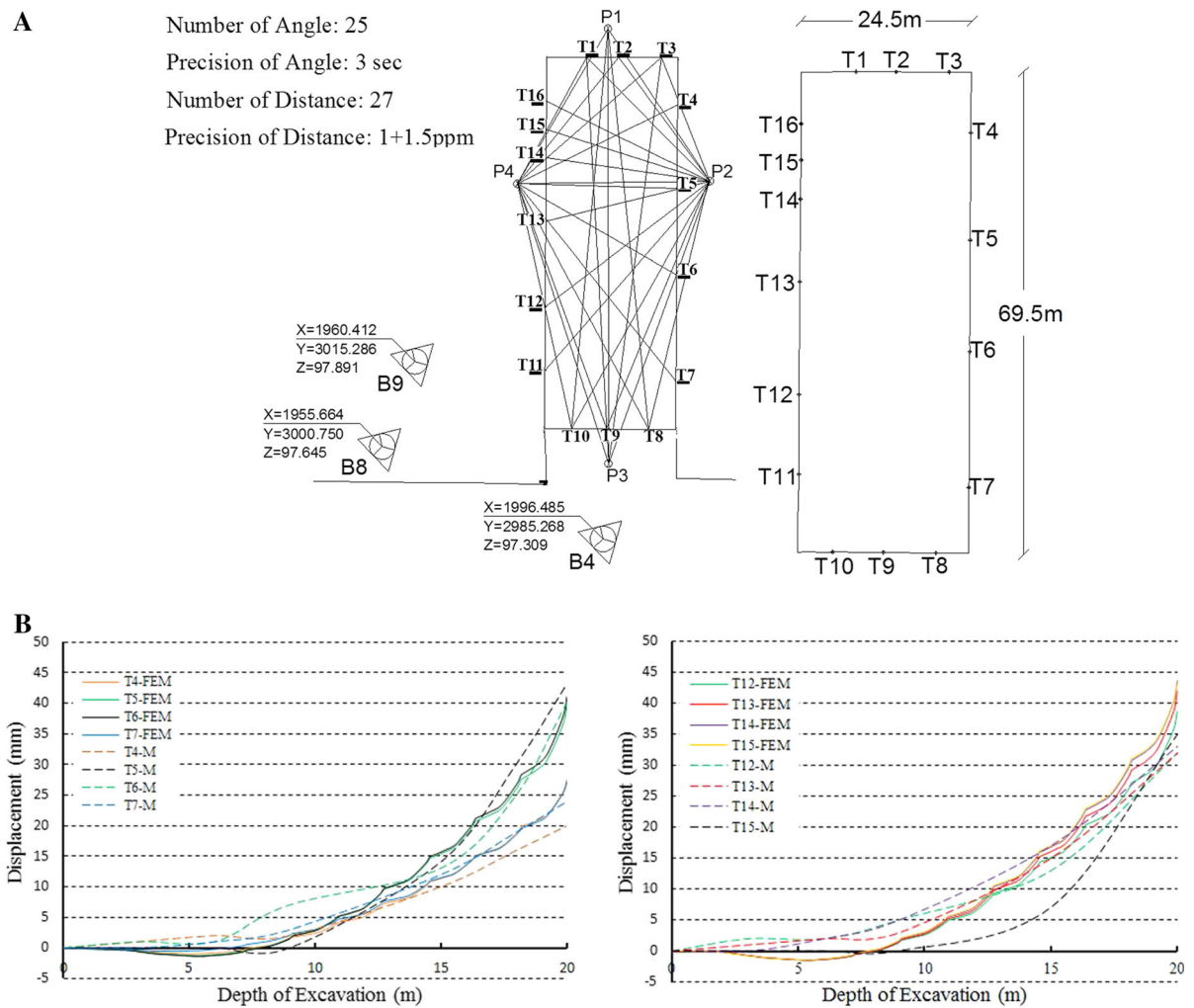


**Fig. 4** **a** Monitoring network, **b** comparison between results of FE model and monitoring data

properties defined based on results of in-situ tests. Concrete damage plasticity constitutive model was used to simulate masonry unit response. This constitutive model is a continuum, plasticity-based, damage model for concrete and similar materials. In this regard, the main two failure mechanisms are as tensile cracking and compressive crushing of the concrete material. The evolution of the yield (or failure) surface is controlled by two hardening variables, linked to failure mechanisms under tension and compression loading, respectively. Figure 5 shows typical views of instrumented BW and corresponding FE models.

## 5 Numerical Results and Discussion

An overview to data collected from case studies (Fig. 1) shows the uncertainties and scattering in damage levels of BWs in the space of “displacement ratio” and “normalized distance”. Thus, numerical analysis and parametric studies were performed to prepare a framework to manage data and carry out more analyses on outputs of case studies. To create the framework, by considering DPI criterion, it is attempted to investigate damage severity variation in EAD using numerical simulations.



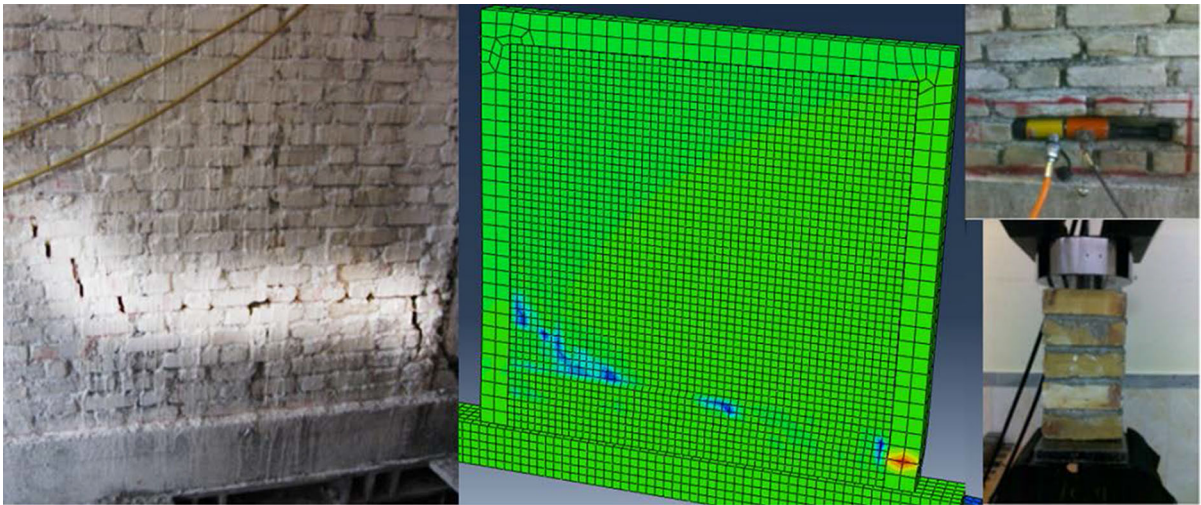


**Fig. 5** Some views of the BW model and instrumented BW (Instrumented BW was constructed by Shakib et al. 2013)

**Table 7** Properties of soil types assigned to FE model

Soil Label	C (kN/m <sup>2</sup> )	$\varphi$ (degree)	$E_0$ (kN/m <sup>2</sup> )	$E_{un/re}$ (kN/m <sup>2</sup> )	$\nu$	$\Gamma$ (kN/m <sup>3</sup> )
S1	40	20	3e4	9e4	0.35	19
S2	20	33	4e4	1.2e5	0.3	20
S3	10	36	6e4	1.8e5	0.3	20
S4	20	33.5	3e4	9e4	0.31	20.8
S5	30	29	4.2e4	1.26e5	0.3	20
S6	12	34	5.5e4	1.65e5	0.3	21
S7	10	31	3.8e4	11.4e5	0.3	20
S8	5	34	5e4	1.5e5	0.3	20

C Cohesion,  $\varphi$  Friction angle,  $E_0$  Elastic modulus,  $E_{un/re}$  Unloading/reloading elastic modulus,  $\nu$  Poisson ration,  $\gamma$  Unit weight

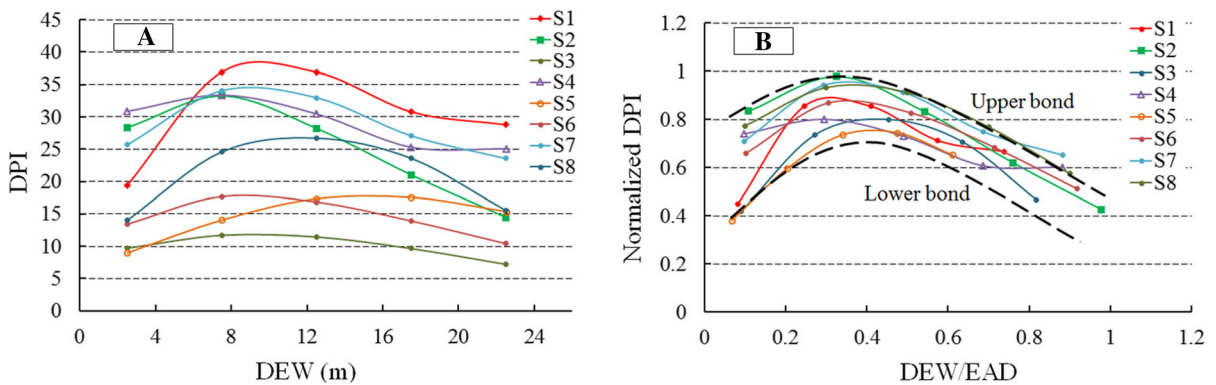


**Fig. 6** a Variation of DPI versus DEW, b variation of normalized DPI versus DEW/EAD

### 5.1 Variation of Damage Level in EAD

Adopting methodology mentioned in Sect. (4), FE models of SNW were developed and FE model of BW was imported to SNW model and put in different

distances of excavation wall in EAD. Distances between BW (center of BW) and SNW for different models were considered as 2.5, 7.5, 12.5, 17.5, and 22.5 m. In the following, eight types of soil properties were assigned to the FE models (Table 7). In each FE

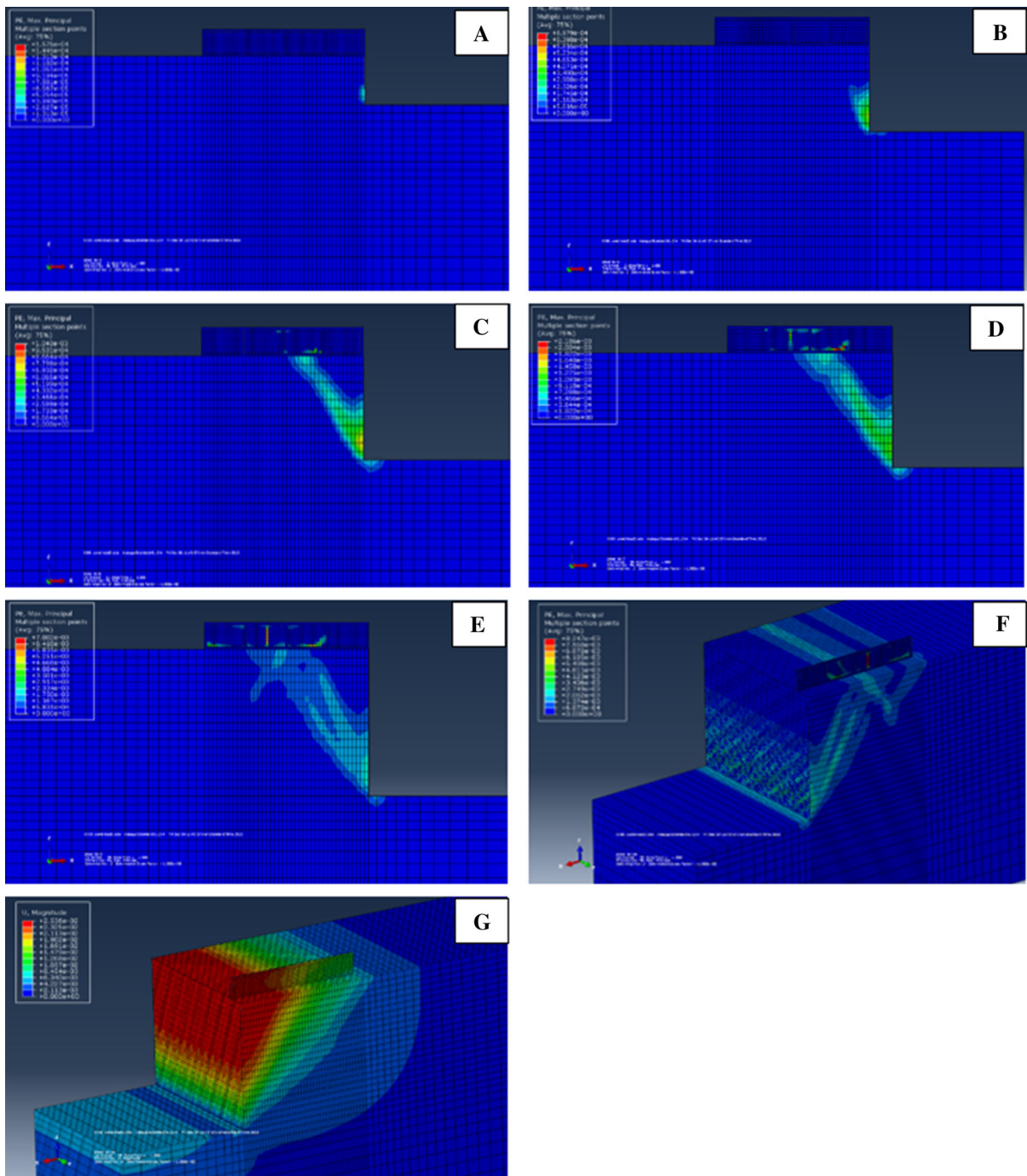


**Fig. 7** Development of plastic points in supported soil and adjacent BWs

model, damage levels were evaluated numerically by calculating DPI using Eq. 1. Deformation parameters ( $U$  and  $V$ ) referred in Eqs. 3 and 4, are extracted directly from FE models. Variation of DPI for

different soil types (Table 7) is shown in Fig. 6a. In this figure, DEW is distance from excavation wall. The results in Fig. 6a show that outputs are significantly scattered. To reduce this scattering, DEW and DPI

**Table 8** Explanation of sub-figures A to G in Fig. 7

Figure no	Depth (m)	Specifications	Description
A	6	Plastic points	Initiation of plastic points in supported soil
B	10	Plastic points	Enhancement of plastic area in supported soil
C	12	Plastic points	Extension of plastic points to the surface + crack initiation of BWs
D	16	Plastic points	Creation of plastic bond in supported soil
E	20	Plastic points	Extension of cracks in BWs
F	20	Plastic points	3D view of plastic points in soil and crack generation in BWs
G	20	Total displacement	Total displacement of supported soil and BWs

were normalized to Excavation Affected Distance (EAD) and maximum wall deflection (in mm), respectively (Fig. 6b). EAD for each model is estimated on basis of the performed numerical analysis. Based on the results shown in Fig. 6b, it can be concluded that by going far from excavation wall, damage level slightly increases and decreases rapidly thereafter. It is also implied that higher levels of damage are likely to occur in a distance 0.3 to 0.5 times of EAD from excavation wall. Upper bond and lower bond of outputs are also depicted in the figure.

To scrutinize variation of damage level versus DEW, the plastic points in supported soil and adjacent BWs during the excavation progress were developed and presented. In the presented case, excavation depth is equal to 20 m, nails length are 14 m in a uniform pattern, and the total length of BWs is equal to 20 m (4 BWs with the length of 5 m). Soil type with label S5 was selected as the geotechnical situation. Development of plastic points in supported soil and adjacent BWs could be seen in Fig. 7. Description of each sub-figures is presented in Table 8. The same as results concluded from Fig. 6, it can be seen that by going far from excavation wall, damage level increases and then decreases. Location of maximum damage level in BWs is affected by shear strain bond position in supported soil.

Location of shear strain bond mostly depend on the soil properties. Cohesion and friction angle are the most important factors that define the shear bond position. Figure 8 clarifies the effects of soil type on

plastic points generation in shear bond. In this figure, plastic points have been presented at the final stage of excavation process for three types of soil: cohesive, frictional and cohesive-frictional. The selected parameters have been tagged to the pictures. As shown in the figure, by increasing the friction angle of the soil, position of shear strain bond recedes from the wall face.

## 5.2 Pattern of DPI Variation in EAD (Deterministic Approach)

In addition to variation of soil types, three types of nail arrangement (as shown in Fig. 9) with two horizontal nail spacing (1.5 m and 2 m) were used to follow the parametric study. Minimum safety factor for different failure modes was considered greater than 1.35 for all SNW models (Lazarte et al 2003). Different types of soil and nail arrangement lead to different values of excavation wall deformation and correspondingly, different damage levels in EAD. Main outputs of numerical studies are summarized in Fig. 10a. In this figure, variation of DPI is depicted against variation of Displacement Ratio (DR) and Normalized Distance (ND). Definition of DR and ND is the same as those introduced in case studies. It can be concluded from Fig. 10a that by increasing the distance from excavation wall, the damage level slightly increases and decreases rapidly thereafter. The near linearly increase of DPI by increasing the DR is another result derived from the figure. To have better extension of FEM

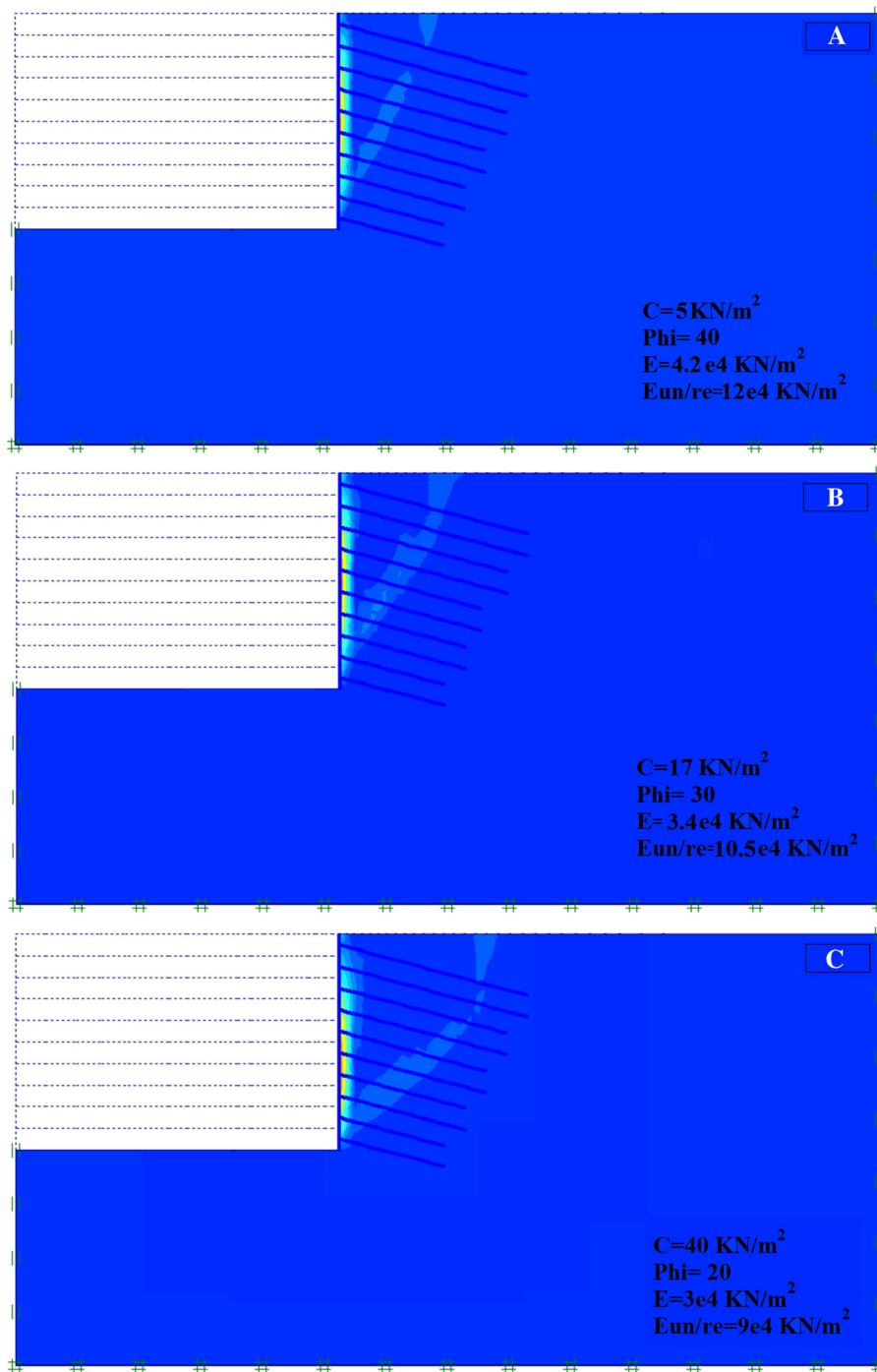


**Fig. 8** The effects of soil type on plastic points generation in the shear bond: **a** Frictional Soil; **b** Frictional-Cohesive soil; **c** Cohesive soil

outputs, a surface is trended through them as shown in Fig. 10b. Regression of trend surface is presented in Table 9.

R-Squared is a statistical measure that represents the proportion of the variance for a dependent variable that's explained by an independent variable or

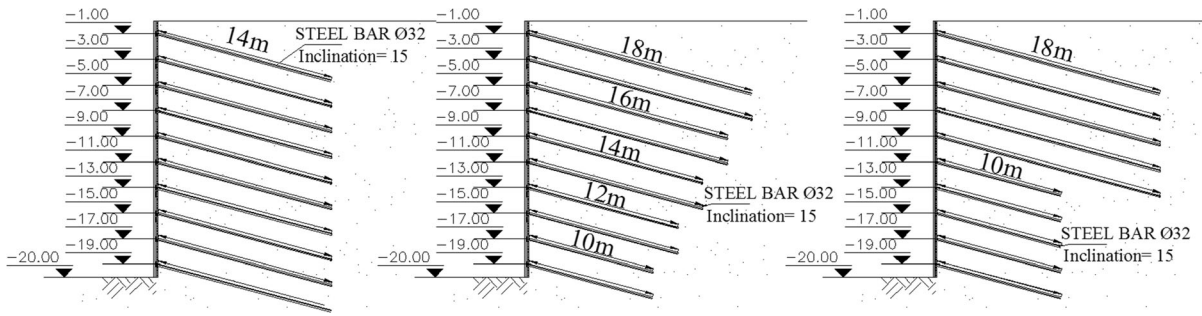


**Fig. 9** Different arrangement of soil nail wall

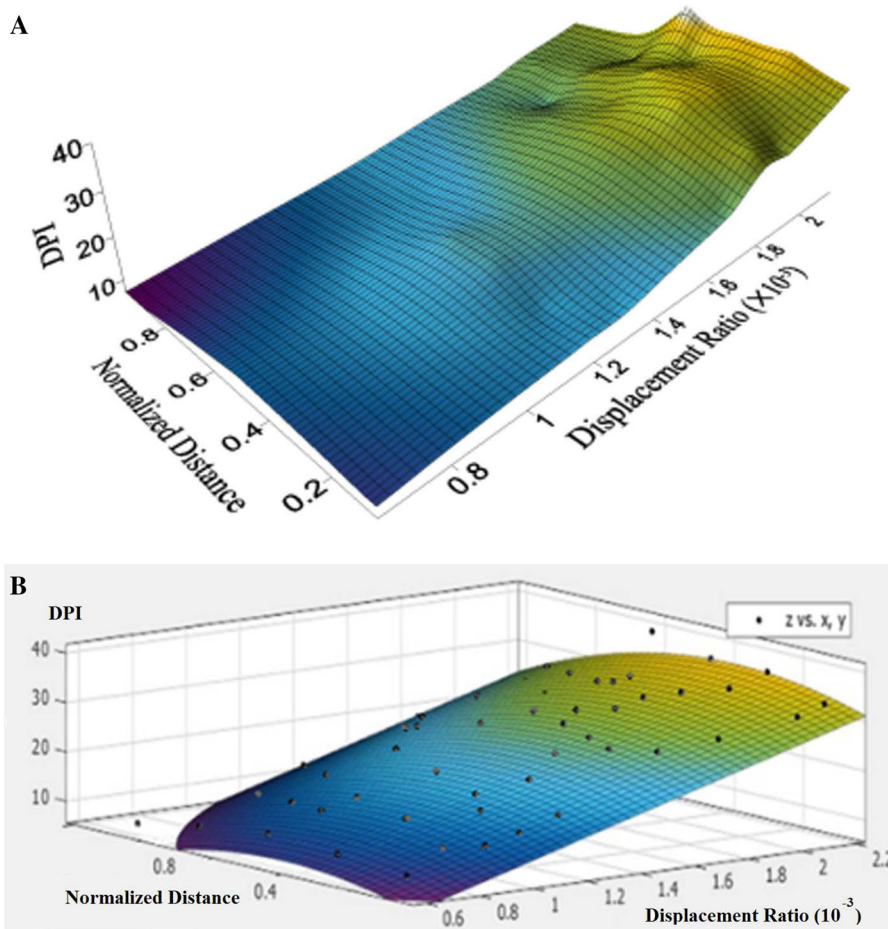


**Fig. 10** **a** Variation of DPI against variation of Displacement Ratio (DR) and **b** Normalized Distance (ND) based on FEM outputs

variables in a regression model. An R-squared of 100% means that all movements of a dependent variable are completely explained by movements in the independent variable. In this study a value of 0.8862 shows good coordination between data and trending surface. SSE is the sum of the squared

differences between each observation and its group’s mean. It can be used as a measure of variation within a cluster. RMSE is the square root of the variance of the residuals. It indicates the absolute fit of the model to the data. Acceptable rang of SSE and RMSE depends on the total range of datum and varies for different

**Table 9** Regression of trend surface through outputs of numerical analysis

Description	R-square	Adj R-sq	SSE	RMSE	Validation SSE	Validation RMSE
Value	0.8862	0.8767	347.3	3.1	347.31	2.95

SSE sum of squares due to error, RMSE root-mean-square error

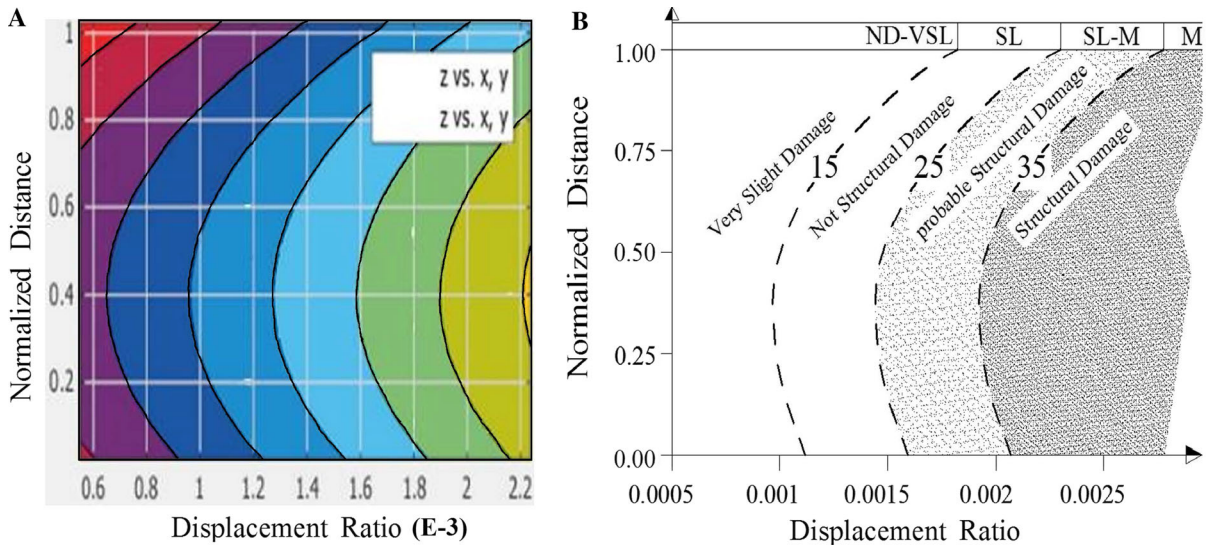


**Fig. 11** a Contour lines of DPI in the space of displacement ratio (DR) and normalized distance (ND), b Limits of different damage levels based on Table 3

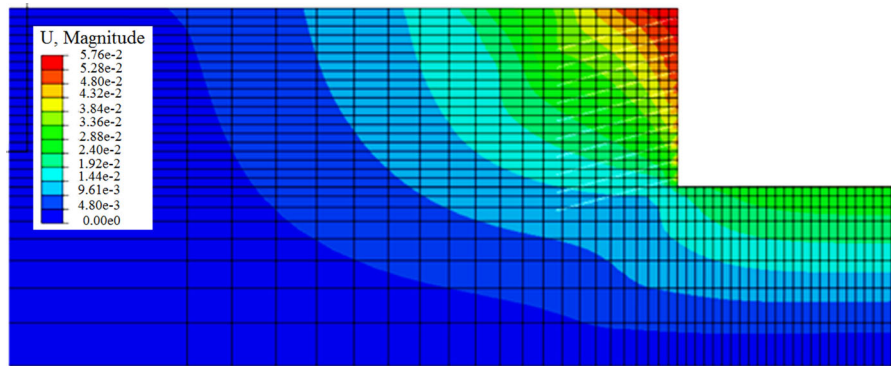


**Fig. 12** Typical views of FE models for estimating the EAD

cases. In this study, the presented values of SSE and RMSE have been accepted by considering the problem situation. By crossing horizontal planes through constant values of DPI in Fig. 10b, different curves with constant DPI could be produced, as shown in Fig. 11a. In this figure, the space between DR and ND is classified into strip areas, for which the values of

DPI in each area are close together. The trend resulted from this figure will be used in Sect. 6 to manage data obtained from case studies (Fig. 1). It must be mentioned that, DR and ND in Fig. 11a are the same as those presented in Fig. 1.

Limits of different damage levels based on Table 1 are mapped to the Fig. 11a, as shown in Fig. 11b. In

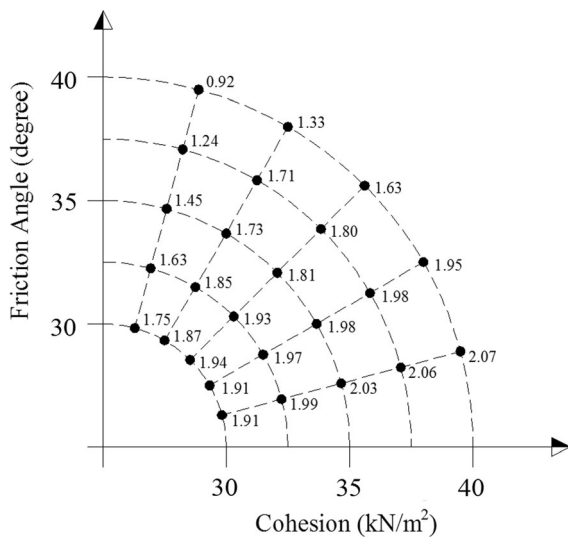


**Fig. 13** Estimation of EAZ distance (i.e. EAD) based on soil cohesion and friction angle

Fig. 11b, the space between displacement ratio and normalized distance is classified into four areas which are in correspondence with Schuster (2009) criteria presented in Table 3. Narrow band in upper part of the figure shows the label of predicted damage levels in the proposed chart.

By considering SL level as the limit of structural damage (Juang et al. 2011), chart area could be classified into area of not structural damage, probable structural damage and structural damage. Using Fig. 11b, it is possible to assess damage level based on two key parameters including: displacement ratio and normalized distance. Presented results can be verified using data presented in Fig. 1. Based on results, by measurement the distance of building from excavation wall and estimation of EAD, normalized distance could be calculated. By computing maximum wall displacement, expected damage level could be assessed according to Fig. 11b.

### 5.3 Estimation of EAD

Excavation Affected Distance (EAD) is used for calculating the “displacement ratio” and “normalized distance”. EAD could be assessed by performing numerical analysis of soil nail wall. In order to obtain an estimation of EAD, simple parametric study was conducted using finite element analysis. In parametric study, different combinations of soil cohesion and

friction angle were imported to the finite element models. Based on classic soil mechanic, parameters  $C$  and  $\Phi$  are most important parameters which define the location of shear bond in supported soil. As described recently, EAD is affected from shear bond location in supported soil. Other parameters, such as elastic modulus were selected based on experimental limits presented by Bowles (1988), engineering judgment and using interpolation. Typical views of FE models have been shown in Fig. 12. Staged construction process of the model is presented in Table 4. Figure 13 presents the results of this study, where label of each point denotes the ratio between EAZ distance and depth of excavation. It could be seen that the enhancement of cohesion increases the EAD values while enhancement of friction angle decreases the EAD values.

## 6 Probability of Buildings Damage

To evaluate probability of buildings damage in EAD,  $P_D$  was obtained using Eq. 5, where,  $P_f \times P_{cdf}$  is calculated instead of calculating  $\sum_y [PL|DR = dr]P[DR = dr]$ . To acquire  $P_{cdf}$ , best-fitted probability density functions were trended through TMS histogram (Fig. 14a) and cumulative distribution function was produced by integration of probability density function, as shown in Fig. 14b. By calculating  $P_{cdf}$  from cumulative distribution function and  $P_f$  from Eq. 6,  $P_D$  was obtained using Eq. 5. Results are shown in Fig. 15a, b.

Figure 15a, b show the damage probability up to VSL and SL levels based on DR, respectively. For example, if the value of DR reaches 0.001, the probable damage in adjacent masonry building up to VSL level (crack width < 1 mm) will be 20%, while up to SL level (Crack width < 5 mm) it will be 4%. Results of this study could be used to estimate the probability of certain damage level of masonry buildings in EAD. By computing maximum wall displacement, displacement ratio can be assessed. Probability of unfavorable damage can be estimated using Fig. 15a, b. Characterization of damage levels in Fig. 15 (SL or VSL) is presented in Table 2.

**Fig. 14** **a** Probability density functions trended through TMS histogram, **b** Cumulative distribution function calculated from

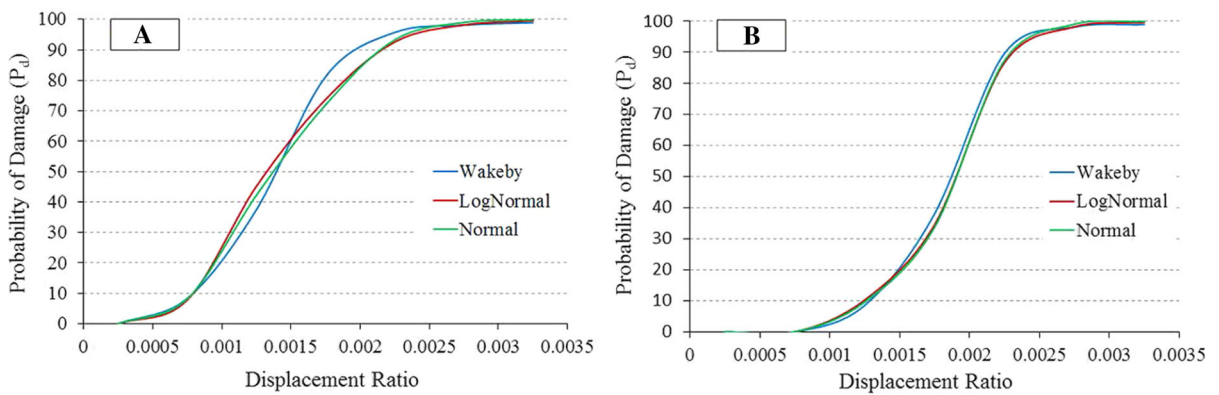
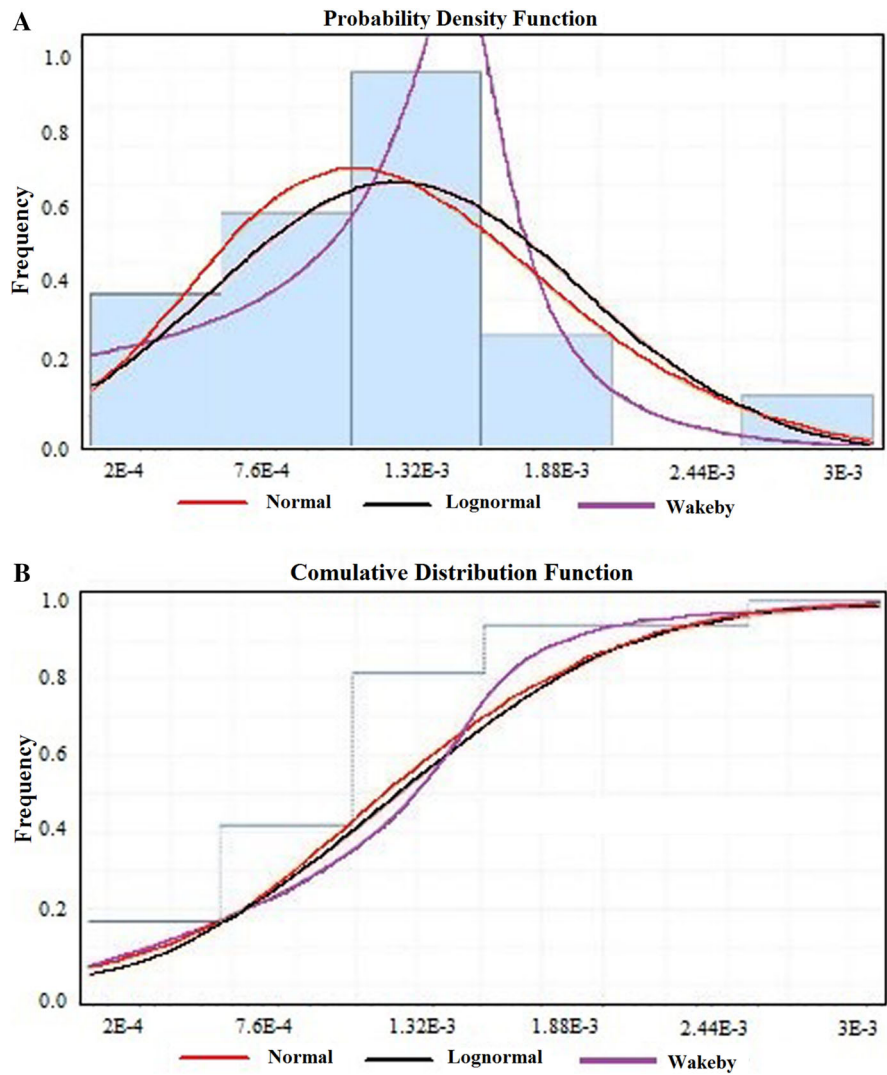


**Fig. 15** Probability of damage up to VSL level (a) and SL level (b) based on DR variation



### 7 Conclusions

This paper is aimed to develop a simple algorithm to estimate the damage probability of masonry buildings in EAD on basis of maximum displacement of SNW. The major findings from this study can be summarized as follows:

1. By increasing the distance from excavation wall, the damage level slightly increases and decreases rapidly thereafter. For masonry buildings, Location of maximum damage level in BWs is followed by shear bond position in supported soil.
2. Using Fig. 11b, it is possible to assess damage level based on two key parameters including: displacement ratio and normalized distance. By measurement the distance of building from excavation wall and estimation of EAD, normalized distance could be calculated. By computing maximum wall displacement, expected damage level could be assessed according to Fig. 11b.
3. To estimate the probability of unfavorable damage to masonry structures in EAD, results shown in Fig. 15a, b can be used. By computing maximum wall displacement, probability of unfavorable damage can be estimated using this figure.

### Appendix

See Table 10.

**Table 10** Summary of measured data from excavation projects in Tehran

No	Reference project	Case	Type of structure	Reported damage	Damage category
C1-1	Andarzgoo Lon: 35° 48' 9" Lat: 51° 27' 26.06"	Wall-A	Masonry	Doors and windows stick slightly	SL
C1-2		Wall-B	Masonry	Fine cracks which can easily be treated	VSL
C1-3		Wall-C	Masonry	Fine cracks which can easily be treated	VSL
C2-1	Amir Kabir Lon: 51° 25' 37.09" Lat: 35° 48' 27.61"	Wall-A	Masonry	Windows and door frames distorted	SE
C2-2		Wall-B	Masonry	Windows and door frames distorted	SE
C2-3		Wall-C	Masonry	The cracks require some opening up and can be patched by a mason	M
C3-1	Yas Hengam Lon: 51° 29' 39.3" Lat: 35° 44' 27.384"	Wall-A	Masonry	Doors and windows stick slightly	SL
C3-2		Wall-B	Masonry	Doors and windows sticking	M

Table 10 continued

No	Reference project	Case	Type of structure	Reported damage	Damage category
C3-3		Wall-C	Masonry	Doors and windows stick slightly	SL
C4-1		Wall-A	Masonry	Doors and windows stick slightly	SL
C4-2		Wall-B	Masonry	The cracks require some opening up and can be patched by a mason	M
C4-3		Wall-C	Masonry	The cracks require some opening up and can be patched by a mason	M
C5-1	Royal	Wall-A	Masonry	The cracks require some opening up and can be patched by a mason	M
	Lon: 51° 23' 18.06"				
	Lat: 35° 43' 14.08"				
C5-2		Wall-B	Masonry	The cracks require some opening up and can be patched by a mason	M
C6-1	Sadr	Wall-A	Masonry	The cracks require some opening up and can be patched by a mason	M
	Lon: 51° 26' 8.73"				
	Lat: 35° 46' 58.65"				
C6-2		Wall-B	Masonry	Doors and windows stick slightly	SL
C6-3		Wall-C	Masonry	Doors and windows stick slightly	SL
C6-4		Wall-D	Masonry	Doors and windows sticking	M
C7-1		Wall-A	Masonry	Cracks easily filled	SL
C7-2		Wall-B	Masonry	The cracks require some opening up and can be patched by a mason	M
C7-3		Wall-C	Masonry	The cracks require some opening up and can be patched by a mason	M
C8-1	Valiasr	Wall-A	Masonry	Cracks easily filled	SL
	Lon: 51° 24' 41.04"				
	Lat: 35° 44' 44.74"				
C8-2		Wall-B	Masonry	Cracks easily filled	M
C8-3		Wall-C	Masonry	Cracks easily filled	SL
C8-4		Wall-D	Masonry	Cracks easily filled	SL
C9-1		Wall-A	Masonry	Cracks easily filled	SL
C9-2		Wall-B	Masonry	Cracks easily filled	SL
C10-1	Nobonyad	Wall-A	Masonry	Fine cracks which can easily be treated	VSL
	Lon: 51° 28' 37.59"				
	Lat: 35° 47' 30.73"				
C10-2		Wall-B	Masonry	Doors and windows stick slightly	SL
C10-3		Wall-C	Masonry	The cracks require some opening up and can be patched by a mason	M
C11-1	Andarzgoo	Wall-A	Masonry	Doors and windows stick slightly	SL
	Lon: 51° 28' 7.82"				
	Lat: 35° 41' 9.23"				

**Table 10** continued

No	Reference project	Case	Type of structure	Reported damage	Damage category
C11-2		Wall-B	Masonry	Doors and windows stick slightly	SL
C11-3		Wall-C	Masonry	Hairline cracks of than about 0.1 mm	ND
C11-4		Wall-D	Masonry	Hairline cracks of than about 0.1 mm	ND
C12-1	Darya Lon: 51° 22' 25.21" Lat: 35° 45' 22.71"	Wall-A	Masonry	Doors and windows sticking	M
C12-2		Wall-B	Masonry	Doors and windows sticking	M
C12-3		Wall-C	Masonry	Doors and windows sticking	M
C13-1		Wall-A	Masonry	Cracks in external brickwork visible on close inspection	VSL
C13-2		Wall-B	Masonry	Cracks easily filled	SL
C14	Haghani Lon: 51° 25' 37.41" Lat: 35° 45' 29.55"	Wall-A	Masonry	Cracks in external brickwork visible on close inspection	VSL
C15		Wall-A	Masonry	Fine cracks which can easily be treated	VSL
C16-1	Arvin Lon: 51° 25' 37.41" Lat: 35° 45' 29.55"	Wall-A	Masonry	The cracks require some opening up and can be patched by a mason	M
C16-2		Wall-B	Masonry	The cracks require some opening up and can be patched by a mason	M
C16-3		Wall-C	Masonry	Doors and windows sticking	M
C17-1		Wall-A	Masonry	Doors and windows stick slightly	SL
C17-2		Wall-B	Masonry	Doors and windows stick slightly	SL
C17-3		Wall-C	Masonry	Cracks in external brickwork visible on close inspection	VSL
C18	Niyayesh Lon: 51° 24' 32.39" Lat: 35° 46' 21.03"	Wall-A	Masonry	Fine cracks which can easily be treated	VSL
C19-1	Atiye Lon: 51° 21' 47.952" Lat: 35° 45' 56.01"	Wall-A	Masonry	Fine cracks which can easily be treated	VSL
C19-2		Wall-B	Masonry	Hairline cracks of than about 0.1 mm	ND
C19-3		Wall-C	Masonry	Hairline cracks of than about 0.1 mm	ND
C20-1	Alborz Lon: 50°58'17.97" Lat: 35°50'36.56"	Wall-A	Masonry	The cracks require some opening up and can be patched by a mason	VSL

Table 10 continued

No	Reference project	Case	Type of structure	Reported damage	Damage category
C20-2		Wall-B	Masonry	The cracks require some opening up and can be patched by a mason	VSL
C21-1		Wall-A	Masonry	Cracks in external brickwork visible on close inspection	VSL
C21-2		Wall-B	Masonry	Doors and windows stick slightly	VSL

## References

- Baecher GB, Christian JT (2005) Reliability and statistics in geotechnical engineering. Wiley, Hoboken
- Basmaji B, Deck O, Al Heib M (2019) Analytical model to predict building deflections induced by ground movements. *Eur J Environ Civ Eng* 23(3):409–431
- Bowles JE (1988) Foundation analysis and design
- Burland JB, Broms BB, DeMello VFB (1977) Behaviour of foundations and structures: state-of-the-art report. In: Proceedings of the 9th international conference on soil mechanics and foundation engineering, Japanese geotechnical society, Tokyo, Japan, pp 495–546
- Castaldo P, Calvello M, Palazzo B (2013) Probabilistic analysis of excavation-induced damages to existing structures. *Comput Geotech* 53:17–30
- Chang LY, Shen J, Xu ZH (2011) Design and 3D numerical analysis of a deep excavation in close proximity to sensitive properties. *J Railway Eng Soc* 11:011
- Dong Y, Burd HJ, Houlsby GT (2017) Finite element study of deep excavation construction processes. *Soils Found* 57(6):965–979
- Ghahreman B (2004) Analysis of ground and building response around deep excavation in sand. Ph. D. Thesis, Department of civil eng., uni of Illinois
- Goh A (2017) Deterministic and reliability assessment of basal heave stability for braced excavations with jet grout base slab. *Eng Geol* 218:63–69
- Goh A, Xuan F, Zhang W (2013) Reliability assessment of diaphragm wall deflections in soft clays. *Found Eng Face Uncertain*:487–496
- Halim D, Wong KS (2011) Prediction of frame structure damage resulting from deep excavation. *J Geotechn Geoenviron Eng* 138(12):1530–1536
- Helwany S (2007) Applied soil mechanics with ABAQUS applications. Wiley, Hoboken
- Hashemi H, Naeimifar I, Uromeihy A, Yasrobi S (2015) Evaluation of rock nail wall performance in jointed rock using numerical method. *Geotech Geol Eng* 33(3):593–607
- Juang C, Schuster M, Ou C, Phoon K (2011) Fully Probabilistic framework for evaluating excavation-induced damage potential of adjacent buildings. *ASCE J Geotechn Geoenviron Eng* 137(2):130–139
- Korff M, Robert J, Frits AF (2016) Pile-soil interaction and settlement effects induced by deep excavations. *J Geotechn Geoenviron Eng* 142(8):04016034
- Lazarte CA, Victor Elias PE, Espinoza RD, Sabatini PJ (2003) Soil nail walls. Report FHWA0-IF-03-017. Washington, D.C. 20590.
- Lin HD, Truong HM, Dang HP, Chen CC (2014a) Assessment of 3D excavation and adjacent building's Responses with consideration of excavation-structure interaction. *Geotechn Spec Publ ASCE* 242:256–265
- Lin HD, Truong HM, Dang HP, Chen CC (2014b) "Assessment of 3D excavation and adjacent building's Responses with consideration of excavation-structure. *Geotech Spec Publ ASCE* 242:256–265
- Minh TH (2013) Study of excavation behavior and adjacent building response with 3D simulation. Doctoral

- dissertation, Master dissertation, National Taiwan University of Science and Technology
- Naeimifar I (2016) Performance analysis of soil nail walls based on excavation-induced damage. Ph. D. Thesis, Tarbiyat Modares University, Tehran (IN FARSI)
- Orazalin Z, Whittle A, Olsen M (2015) Three-dimensional analyses of excavation support system for the stata center basement on the MIT campus. *ASCE J Geotechn Geoenviron Eng* 141(7):05015001
- Ou CY, Liao JT, Cheng WL (2000) Building response and ground movements induced by a deep excavation. *Geotechnique* 50(3):209–220
- Sawwaf M, Nazir AK (2011) The effect of deep excavation-induced lateral soil movements on the behavior of strip footing supported on reinforced sand. *J Adv Res* 3(4):337–344
- Schuster M, Kung GTC, Juang CH, Hashash YM (2009) Simplified model for evaluating damage potential of buildings adjacent to a braced excavation. *ASCE J Geotechn Geoenviron Eng* 135(12):1823–1835
- Shakib H, Mousavi M, Rezaei MK, Dardaei S, Ahmadizadeh M (2013) Analytical and experimental seismic evaluation of unreinforced masonry walls retrofitted by Shotcrete and FRP strips. In: 12th Canadian masonry symposium
- Shi C, Zhang YL, Xu WY, Zhu QZ, Wang SN (2013) Risk analysis of building damage induced by landslide impact disaster. *Eur J Environ Civ Eng* 17(sup1):s126–s143
- Singh VP, Babu GS (2010) 2D numerical simulations of soil nail walls. *Geotech Geol Eng* 28(4):299–309
- Son M, Cording EJ (2005) Estimation of building damage due to excavation-induced ground movements. *ASCE J Geotechn Geoenviron Eng* 131(2):162–177
- Son M, Cording EJ (2011) Responses of buildings with different structural types to excavation-induced ground settlements. *ASCE J Geotechn Geoenviron Eng* 137(4):323–333
- Su Y, Li S, Liu S, Fang Y (2017) Extensive second-order method for reliability analysis of complicated geotechnical structures. *Eur J Environ Civ Eng*:1–19
- Sun Y-q, Yang X-j, Yu Z-W (2005) Study on heave of base of soil nailing protection. *Bull Sci Technol* 2
- Wang L, Luo Z, Xiao J, Juang CH (2014) Probabilistic inverse analysis of excavation-induced wall and ground responses for assessing damage potential of adjacent buildings. *Geotech Geol Eng* 32(2):273–285
- Wu D, Wang P, Liu GQ (2013) Influence of C and  $\phi$  values on slope supporting by soil nailing wall in thick miscellaneous fill site. In: *Advanced Materials Research*, vol 706, pp 504–507. Trans Tech Publications
- Wu SH, Ching J, Ou CY (2014) Simplified reliability-based design of wall displacements for excavations in soft clay considering cross walls. *ASCE J Geotechn Geoenviron Eng* 141:3
- Yoo C, Lee D (2008) Deep excavation-induced ground surface movement characteristics: a numerical investigation. *Computers Geotech* 35(2):231–252
- Zevgolis IE, Daffas ZA (2018) System reliability assessment of soil nail walls. *Comput Geotechn*
- Zhang, Zhu WS (2016) Displacement measurement techniques and numerical verification in 3D geomechanical model tests of an underground cavern group. *Tunnel Undergr Space Tech* 56:54–64
- Zhang HB, Chen JJ, Zhao XS, Wang JH, Hu H (2014) Displacement performance and simple prediction for deep excavations supported by contiguous bored pile walls in soft clay. *J Aerosp Eng* 28(6):A4014008
- Zhang W, Goh AT, Zhang Y (2015a) Probabilistic assessment of serviceability limit state of diaphragm walls for braced excavation in clays. *ASCE-ASME J Risk Uncertain Eng Syst Part A Civ Eng* 06015001
- Zhang W, Goh AT, Xuan F (2015b) A simple prediction model for wall deflection caused by braced excavation in clays. *Comput Geotech* 63:67–72
- Zheng G, Xinyu Y, Haizuo Z, Yiming D, Jiayu S, Xiaoxuan Y (2018) A simplified prediction method for evaluating tunnel displacement induced by laterally adjacent excavations. *Comput Geotech* 95:119–128

**Publisher's Note** Springer Nature remains neutral with regard to jurisdictional claims in published maps and institutional affiliations.